April 2000

X-ray structure of the quinoprotein ethanol dehydrogenase from *Pseudomonas aeruginosa*: basis of substrate specificity

Thomas Keitel
Universitätsklinikum Charité Institut für Biochemie Humboldt-Universität zu Berlin, Monbijoustr. 2 D-10117, Berlin, Germany

Annette Diehl
Fachgebiet Technische Biochemie, Institut für Biotechnologie, Technische Universität Berlin, Seestr. 13, D-13353, Berlin, Germany

Tobias Knaute
Universitätsklinikum Charité Institut für Medizinische Immunologie, Humboldt- Universität zu Berlin, Ziegelstr. 3, D- 10117, Berlin, Germany

John J. Stezowski
University of Nebraska - Lincoln, jstezowski1@unl.edu

Wolfgang Hohne
Universitätsklinikum Charité Institut für Biochemie Humboldt-Universität zu Berlin, Monbijoustr. 2 D-10117, Berlin, Germany

See next page for additional authors

Published in *Journal of Molecular Biology* 297:4 (April 7, 2000), pp. 961–974. doi:10.1006/jmbi.2000.3603 Available online at http://www.idealibrary.com/

Submitted October 25, 1999; revised February 8, 2000; accepted February 9, 2000; published online April 15, 2002.

X-ray structure of the quinoprotein ethanol dehydrogenase from *Pseudomonas aeruginosa*: basis of substrate specificity

Thomas Keitel [1, 2], Annette Diehl [2], Tobias Knaute [3], John J. Stezowski [4], Wolfgang Höhne [1], and Helmut Görisch [2,*]

[1] *Universitätsklinikum Charité Institut für Biochemie Humboldt-Universität zu Berlin, Monbijoustr. 2 D-10117, Berlin, Germany*

[2] *Fachgebiet Technische Biochemie, Institut für Biotechnologie, Technische Universität Berlin, Seestr. 13, D-13353, Berlin, Germany*

[3] *Universitätsklinikum Charité Institut für Medizinische Immunologie, Humboldt-Universität zu Berlin, Ziegelstr. 3, D-10117, Berlin, Germany*

[4] *Department of Chemistry University of Nebraska, Lincoln, NE 68588-0304, USA*

** Corresponding author. Email:* goerisch@lb.TU-Berlin.de

Abstract: The homodimeric enzyme form of quinoprotein ethanol dehydrogenase from *Pseudomonas aeruginosa* ATCC 17933 crystallizes readily with the space group *R*3. The X-ray structure was solved at 2.6 Å resolution by molecular replacement.

Aside from differences in some loops, the folding of the enzyme is very similar to the large subunit of the quinoprotein methanol dehydrogenases from *Methylobacterium extorquens* or *Methylophilus* W3A1. Eight W-shaped β-sheet motifs are arranged circularly in a propeller-like fashion forming a disk-shaped superbarrel. No electron density for a small subunit like that in methanol dehydrogenase could be found. The prosthetic group is located in the centre of the superbarrel and is coordinated to a calcium ion. Most amino acid residues found in close contact with the prosthetic group pyrroloquinoline quinone and the Ca^{2+} are conserved between the quinoprotein ethanol dehydrogenase structure and that of the methanol dehydrogenases. The main differences in the active-site region are a bulky tryptophan residue in the active-site cavity of methanol dehydrogenase, which is replaced by a phenylalanine and a leucine side-chain in the ethanol dehydrogenase structure and a leucine residue right above the pyrrolquinoline quinone group in methanol dehydrogenase which is replaced by a tryptophan side-chain. Both amino acid exchanges appear to have an important influence, causing different substrate specificities of these otherwise very similar enzymes. In addition to the Ca^{2+} in the active-site cavity found also in methanol dehydrogenase, ethanol dehydrogenase contains a second Ca^{2+}-binding site at the N terminus, which contributes to the stability of the native enzyme.

Keywords: quinoprotein; ethanol dehydrogenase; *Pseudomonas aeruginosa*; X-ray crystallography; substrate specificity

Abbreviations: QEDH, quinoprotein ethanol dehydrogenase; QMDH, quinoprotein methanol dehydrogenase; PQQ, pyrroloquinoline quinone

Introduction

The vast majority of microbial alcohol dehydrogenases are NAD(P)-dependent enzymes and occur in the cytoplasm. However, a number of Gram-negative bacteria oxidizing alcohols or aldoses produce enzymes that contain the prosthetic group pyrroloquinoline quinone (PQQ) [Goodwin and Anthony 1998]. These quinoprotein alcohol dehydrogenases are either soluble enzymes of the periplasm or are membrane-bound, being oriented towards the periplasmic space [Matsushita and Adachi 1993]. Among the quinoprotein-type alcohol dehydrogenases, enzymes have been described that are induced by and act preferentially on methanol [Anthony 1993], ethanol [Gorisch and Rupp 1989], glycerol [Toyama et al 1995], polyvinylalcohol [Shimao et al 1986], or shikimate [van Kleef and Duine 1988].

The *Journal of Molecular Biology* version of this article was edited by D. C. Rees.

Authors' present addresses: T. Keitel, MPI für Medizinische Forschung, Jahnstr. 29, D-69120 Heidelberg, Germany; A. Diehl, Forschungsgruppe Kristallographie, Max-Delbrück-Zentrum für Molekulare Medizin, Robert-Rössle-Str. 10, 13092 Berlin, Germany.

The best studied example of the PQQ-dependent dehydrogenases is the quinoprotein methanol dehydrogenase (QMDH) isolated from a number of methylotrophic bacteria. These soluble enzymes are heterotetramers of two large (60-66 kDa) and two small (8.5-10 kDa) subunits. QMDHs show a pH optimum above 9, and require ammonia or an alkylamine for activity. They oxidize methanol with a K_m value in the micromolar range. Other primary alcohols are oxidized, but secondary alcohols are not attacked [Anthony 1986].

X-ray structures of QMDH have been determined for the enzymes isolated from *Methylophilus methylotrophus* and *Methylophilus* W3A1 [White et al 1993, Xia et al 1992, Xia et al 1996 and Xia et al 1999] and from *Methylobacterium extorquens* [Anthony et al 1994, Ghosh et al 1994 and Ghosh et al 1995]. The large subunit of QMDH is folded into eight twisted β-sheets, which, in a propeller-like fashion, form a disk-shaped superbarrel [Branden and Tooze 1991], the so-called β-propeller structure [Murzin 1992]. A regular interaction between propeller blades is formed by a tryptophan docking motif, where usually an alanine, a tryptophan and a glycine residue establish close van der Waals contacts [Ghosh et al 1995].

The PQQ is located in the centre of the superbarrel structure and is accessible from the surface through a hydrophobic funnel ending in a small channel. The prosthetic group is embedded between an unusual disulphide ring formed by two adjacent cysteine residues and the indole ring of a tryptophan residue. In addition, it forms several equatorial hydrogen bridges *via* its carboxyl groups to surrounding protein residues and is coordinated to a calcium ion.

A similar eight-bladed β-propeller fold has been described for nitrite reductase from *Thiosphaera pantotropha*, with heme as the prosthetic group [Baker et al 1997]. In addition, there are proteins that form seven-bladed propeller, six-bladed propeller, and even four-bladed β-propeller domains [Renault et al 1998, Janakiraman et al 1994 and Gomis et al 1996]. All these proteins do not share significant overall sequence homology with each other or quinoprotein alcohol dehydrogenases.

Another type of PQQ-dependent alcohol dehydrogenases induced by ethanol has been found in several *Pseudomonas* strains [Gorisch and Rupp 1989, Toyama et al 1995 and Rupp and Gorisch 1988] and in *Rhodopseudomonas acidophila* [Bamforth and Quayle 1979]. These quinoprotein ethanol dehydrogenases (QEDHs) show enzymatic and molecular properties similar to those of the QMDHs from methylotrophs. The two groups of enzymes differ in their substrate specificity. The QEDHs oxidize primary alcohols and, in contrast to QMDHs, attack also secondary alcohols, but methanol is a poor substrate due to its high K_m value [Anthony 1986]. In addition, the QEDHs appear to be homodimers of 60 kDa subunits [Gorisch and Rupp 1989 and Toyama et al 1995] in contrast to the heterotetrameric structure of QMDHs, which are composed of two large and two small polypeptides. The function of the small subunit in QMDH is unknown. Despite an earlier report, that QEDH from *Pseudomonas aeruginosa* also contains a small 9 kDa subunit [Schrover et al 1993], we demonstrated recently that the cloned gene encoding the 65 kDa subunit of QEDH is expressed in *Escherichia coli* as an enzymically active form in the absence of a 9 kDa peptide, confirming an α_2 structure [Diehl et al 1998]. In contrast, formation of active QMDH requires expression of its small polypeptide, which is tightly bound to the large subunit [Nunn et al 1989].

The deduced amino acid sequence of QEDH from *P. aeruginosa* is homologous to other known quinoprotein alcohol dehydrogenases. When compared with QMDH, the typical tryptophan docking motifs were found, and it was predicted that QEDH will show a very similar overall folding resulting in a propeller-like superbarrel. Also, the two adjacent cysteine residues forming an eight-membered disulphide ring and the tryptophan being in close contact with the prosthetic group PQQ in the *M. extorquens* and *M.* W3A1 QMDHs are conserved in the *P. aeruginosa* QEDH as well [Diehl et al 1998].

With QEDH from *P. aeruginosa* [Mutzel and Gorisch 1991] and the PQQ-dependent glucose dehydrogenase from *Acinetobacter calcoaceticus* [Geiger and Gorisch 1989] it was demonstrated for the first time, that these quinoproteins contain stoichiometric amounts of Ca^{2+} with respect to the prosthetic group PQQ.

Besides the *Pseudomonas* ethanol dehydrogenases, there are other types of quinoprotein alcohol dehydrogenases that are induced by ethanol. Acetic acid bacteria produce a membrane- bound quinohemoprotein alcohol dehydrogenase [Matsushita and Adachi 1993], while a soluble monomeric quinohemoprotein ethanol dehydrogenase was isolated from *Comamonas testosteroni* [de Jong et al 1995]. Model structures of the acetic acid bacterial type [Cozier et al 1995] and the *Comamonas* type [Jongejan et al 1998] of quinohemoproteins have been built by homology modeling based on the structure of the α-subunit of QMDH.

QEDH from *P. aeruginosa* readily crystallized in the presence of $(NH_4)_2SO_4$ or polyethyleneglycol [Gorisch and Rupp 1989] and crystals formed were suitable for X-ray diffraction studies, which allowed determination of the space group and unit cell constants [Stezowski et al 1989]. Here, we report the solution of the three-dimensional structure of QEDH from *P. aeruginosa* by the method of molecular replacement. The structure is compared with that of QMDH. The differences in the substrate specificity of QMDH and QEDH are explained by structural differences in the cavity accommodating the substrate in the vicinity of the prosthetic group PQQ.

Results and discussion

Solution of the structure

A complete data set was collected from a single crystal of QEDH. The asymmetric unit is occupied by a dimeric molecule consisting of two identical subunits. The packing density was calculated to 2.5 Å^3/Da (51 % (v/v) solvent). Further crystallographic information is given in Table 1.

The structure was solved at 2.6 Å by the method of molecular replacement using the structure of QMDH from the methylotrophic bacterium *Methylophilus* W3A1 [Xia et al 1992 and Xia et al 1996] which shows about 30 % identical positions in the sequence alignment with QEDH. The resulting electron density was interpreted using the sequence data for QEDH [Diehl et al 1998]. The structure was refined to an *R*-factor of 19.2 % and an R_{free}-factor of 27.4 % with 106 water molecules included per dimer, all with reasonable binding geometry to the protein. In both subunits, electron density is missing for the last seven residues (Asp583 to Arg589), and only weak electron density was found in the loop regions 229-237, 279-285, 329-334 and 395-398, which are not involved in the tight interaction network of the protein β-sheet core and thus are highly flexible (Scheme 1). Definitely no electron density was found for a putative small β-subunit.

The packing of the 65 kDa subunits in QEDH crystals is such that the site of the small subunit in the QMDH structure is occupied by a symmetrically equivalent 65 kDa subunit in QEDH. In addition, there is no electron density elsewhere to account for a small subunit like that in QMDH.

The phi/psi angles fall into the allowed regions of the Ramachandran plot: 80.5 % in the most favoured regions, 17.6 % in additionally allowed regions and 1.7 % in generously allowed regions [Ramachandran and Sasisekharan 1968]. Only Asp107 in every subunit is forced into an unusual geometry by the disulphide ring of the two adjacent residues Cys105 and Cys106.

Overall description of the structure

The overall structure of QEDH from *P. aeruginosa* shows the typical eight-bladed β-propeller fold as seen in the X-ray structures of homologous QMDHs from *M.*W3A1 or *M. extorquens* (Figure 1) [Ghosh et al 1995, White et al 1993, Xia et al 1992, Xia et al 1996 and Ghosh et al 1994]. Each β-propeller blade W_1 to W_8 is formed by four antiparallel β-strands A, B, C and D. Blade W_8 is a composite structure where β-strands A, B and C are donated by the C terminus while strand D stems from the N terminus of the polypeptide (Scheme 1) . A consensus amino acid docking sequence with usually alanine at position 1, glycine at position 7, and tryptophan at position 11 [Anthony and Ghosh 1998 and Diehl et al 1998], is located in the C and D strands of each β-propeller blade, and an array of close van der Waals contacts is formed between residues of the amino acid docking sequences of adjacent β-propeller blades. Typically, a triad consisting of an alanine and tryptophan side-chain of β-strands C and D of blade W_n together with a glycine backbone located in strand D of blade W_{n+1}, form Ala/Trp/Gly tryptophan docking motifs M1 to M8 (Figure 2(a). In addition to the van der Waals contacts

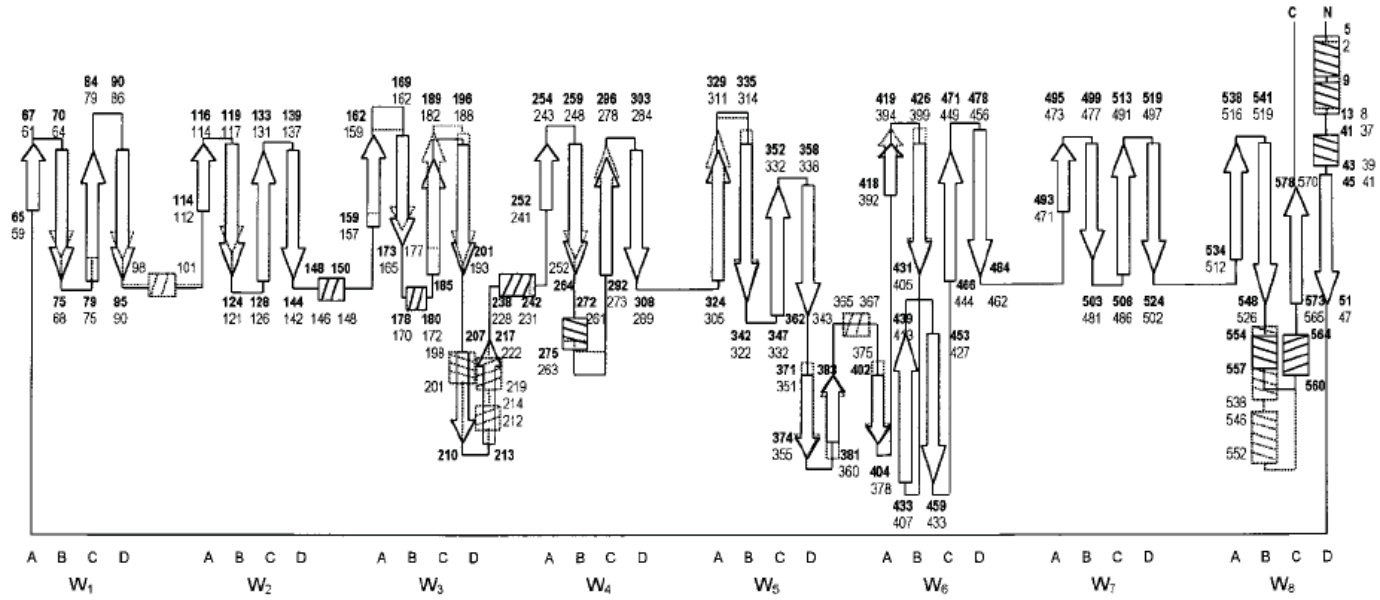

Scheme 1. Comparing the folding scheme for QEDH from *P. aeruginosa* and QMDH from *M.* W3A1 in two dimensional schematic representation. Arrows correspond to β-strands, boxes with diagonals indicate α-helical segments. The numbering refers to the first or last residue of the corresponding secondary structural element. Bold numbers and solid lines represent the QEDH folding scheme; dotted lines refer to QMDH. The eight W-shaped β-propeller folds are indicated by W_1 to W_8 with β-strands A, B, C, and D.

Table 1. Diffraction data statistics and cell constants

Cell parameters	*a*, *b*, *c* (Å)	159.40	159.40	130.95
	α, β, γ (deg)	90	90	120
Space group			R3	
Completeness to 2.6 Å (%)			>98	
Resolution of data measured (Å)			25.6-2.52	
Number of reflections measured			109,117	
Number of unique reflections			40,136	
R_{merge} (%)			12.6	
R_{merge} (%) 2.7-2.6 Å			36	
$\langle F \rangle / \langle \sigma F \rangle$			15	
Average *B*-factor (Å^2)			28.2	
Resolution used for refinement (Å)			12.5-2.6	
R-factor (%)			19.2	
R_{free}-factor (%)			27.4	
Water molecules			106	
Atoms used in refinement			9234	
r.m.s. dev.bond length (Å)			ca 0.013	
r.m.s. dev.bond angles (deg.)			ca 5.00	

$R_{merge} = ((h(i|(\langle I(h) \rangle - I(h)i)|/(h(iI(h)) \times 100$, with $I(h)i$ = observed intensity in the *i*th dataset and $\langle I(h) \rangle$ = mean intensity of reflection *h* over all measurements of $I(h)$. *F* and σF, structure factor amplitude and r.m.s. error of the structure factor amplitude.

of the tryptophan docking motif, the conserved tryptophan residue forms typically a hydrogen bond through the indole NH group with the backbone carbonyl group of residue 4 or 5 in the next amino acid docking sequence in blade W_{n+1}, and a β-sheet hydrogen bond between its carbonyl oxygen atom and the main-chain amide nitrogen atom of residue 1 within the same amino acid docking sequence. A regular repetitive tryptophan docking motif with an Ala/Trp/Gly interaction was described for QMDH and it is assumed that this interaction makes a major contribution to the stability of the β-propeller fold [Anthony and Ghosh 1998 and Xia et al 1996].

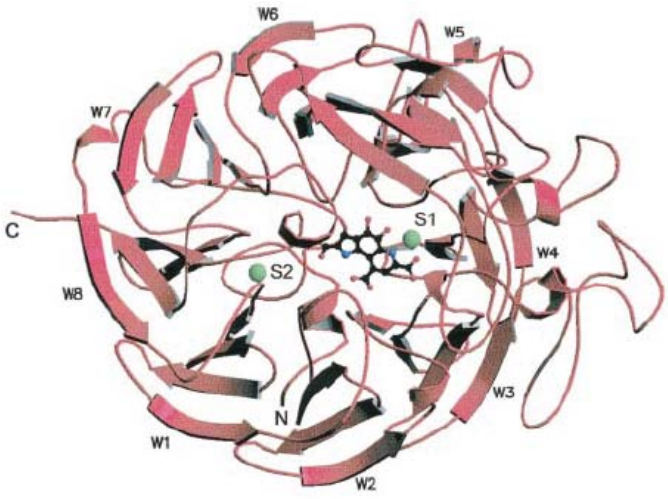

Figure 1. General folding topology of QEDH from *P. aeruginosa* with PQQ in the active-site and the two calcium ions (green) at the PQQ binding site (S1) and at an N-terminal binding site (S2). The eight propeller blades W_1 to W_8 are formed by four antiparallel β-strands A, B, C and D. The A strands are the innermost ones.

In QEDH, modified amino acid docking sequences are found with β-propeller blades W_4, W_5 and W_8 [Diehl et al 1998]. This results in modified tryptophan docking motifs M4, M5, M7 and M8 (Scheme 2) In M4, the expected Ala is replaced by Gly in position 295, but the missing methyl group is contributed by Thr259 (Figure 2(b). The only replacement of a Trp occurs in the typical amino acid docking sequence in W_5at position 360, where Asn is found. The docking interaction in M5 is shifted by two positions to Phe362, which contacts the backbone of Gly476 and uses a hydrophobic interaction with Phe348, instead of contacting Val at position 350, which replaces the regular Ala. In M7, Trp521 forms a contact to the side-chain of Leu44 instead of to a Gly backbone, while in M8, Val at position 576 replaces the expected Ala, making the corresponding hydrophobic contact to Trp48. Interestingly, all modified tryptophan docking motifs in QEDH are close to functionally important sites. Motif W_5 is close to the active-site cavity and motifs W_4, W_7 and W_8 are close to the subunit interface with a network of hydrophobic and hydrogen bond interactions. Similar deviations from the regular docking motif occur in QMDH (Scheme 2).

Even though the common folding scheme of the large α-subunit of QMDH is conserved in QEDH from *P. aeruginosa* (Scheme 1), the course of the backbone is different for some loops, especially in the vicinity of the active-site and in the region where the small subunit binds in QMDH. In QEDH, several loops protrude from the molecule surface and partly occupy the space filled by the small subunit in QMDH (Figure 3). In particular, a loop between residues 204 and 222 is oriented in a different direction. A common feature of those loops in QEDH is their flexibility, which is indicated by rather high *B*-factors and partly discontinuous electron density.

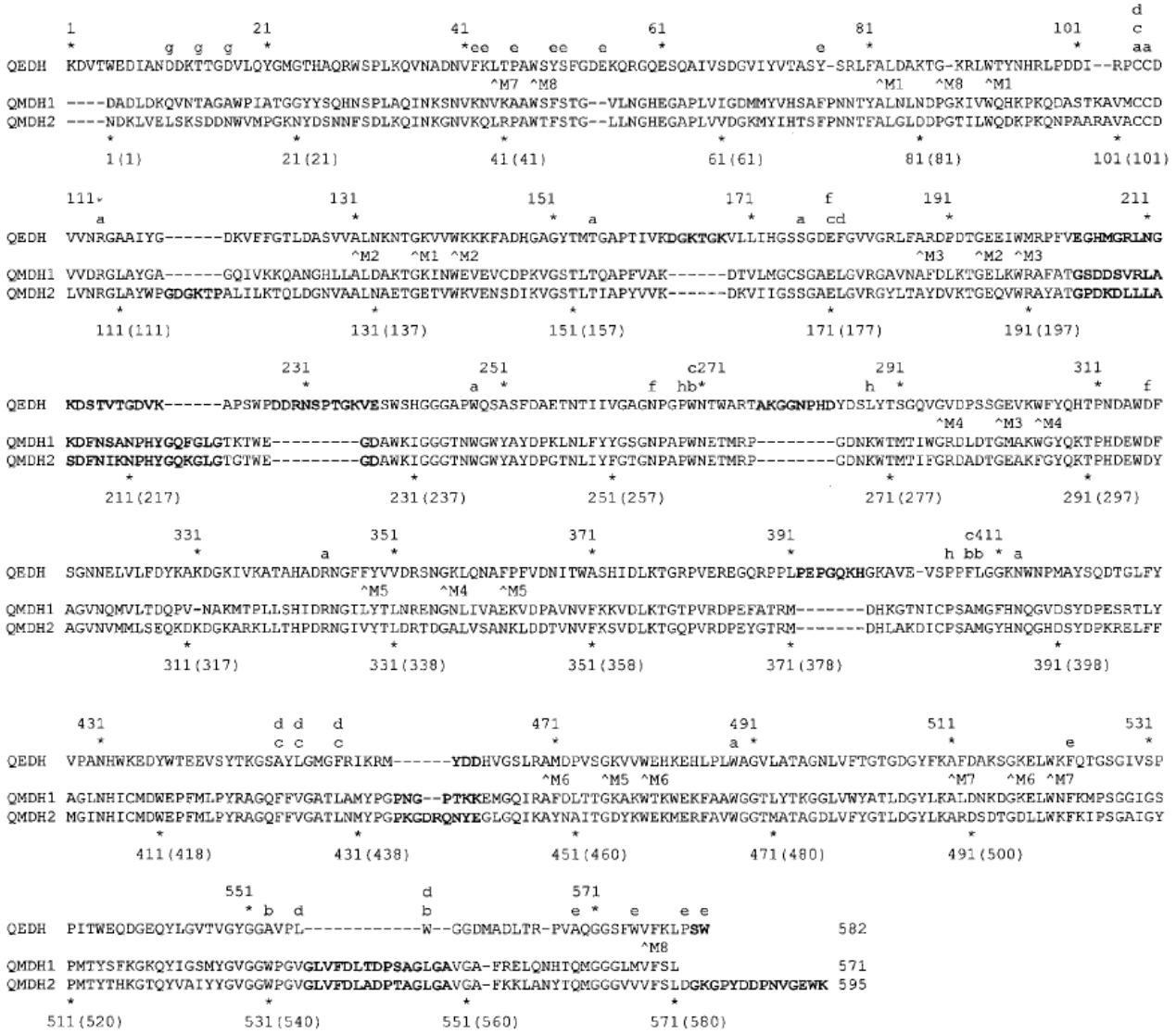

Scheme 2. Sequence alignment and functionally or structurally important positions for ethanol and methanol dehydrogenases with known structure. Alignment according to structurally equivalent residues, larger sequence regions with non corresponding structures in QEDH and QMDH are in bold letters. C-terminal residues not included in the reported X-ray structures are not shown. QEDH: quinoprotein ethanol dehydrogenase from *Pseudomonas aeruginosa* ATCC17933, EMBL Acc No AJ009858; QMDH1: quinoprotein methanol dehydrogenase from *Methylophilus* W3A1, EMBL Acc No U41040; QMDH2: quinoprotein methanol dehydrogenase from *Methylobacterium extorquens*, EMBL Acc No M31108; Numbering above the sequences according to QEDH from *Pseudomonas aeruginosa*, below the sequences according to QMDH from *Methylophilus* W3A1, in parentheses according to QMDH from *Methylobacterium extorquens*. a, side chains in contact with PQQ. b, residues in the active site cavity. c, residues at the active site access. d, residues forming a depression around the entrance to the active site (putative cytochrome c1 docking site). e, side chains involved in subunit interaction. f, Ca^{2+} ligands in the active site cavity. g, second Ca^{2+} site. h, *cis*-peptide bond. M1-8 residues involved in tryptophan docking motifs 1 to 8.

QEDH contains an unusual disulphide bridge of adjacent Cys residues in the active-site. The eight-membered ring system with the Cys105-Cys106 peptide bond in *trans* configuration is found also in QMDH and is typical for this group of alcohol dehydrogenases. However, QEDH lacks an additional disulphide bridge present in QMDH. In the QEDH sequence, Ser405 and Lys434 replace the respective Cys residues in QMDH. A hydrogen bond between the OH group of Ser405 and the carboxyl group of Trp433, and a salt-bridge between Glu403 and Lys434 in QEDH, may compensate for the loss of the structure-stabilizing disulphide bridge. The QMDH from *M*. W3A1 contains even a third disulphide bridge between two cysteine residues at positions 144 and 167, which is not found in any other quinoprotein or quinohemoprotein dehydrogenase oxidizing alcohols.

The three *cis*-peptide bonds found in the structure of QEDH at Pro269, Pro406 and an unusual *cis*-peptide

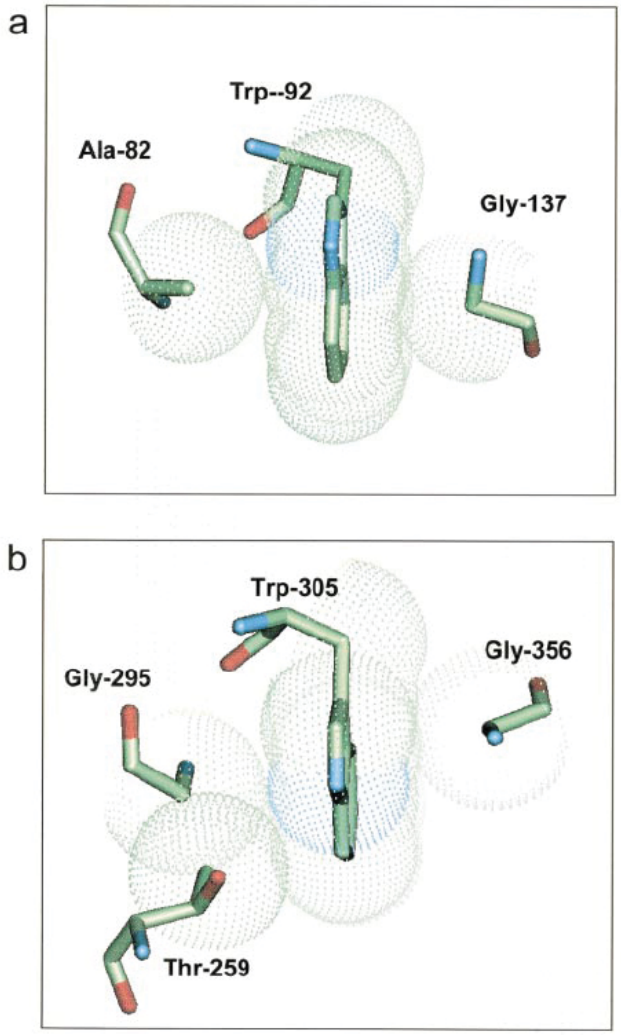

Figure 2. Dot surface/liquorice bond representation of (a) a typical Ala/Trp/Gly docking motif (M1 between W_1 and W_2: Ala82/Trp92/Gly137) and (b) a deviating docking motif (M4 between W_4 and W_5: Gly295, Thr259/Trp305/Gly356).

bond between Leu288 and Tyr289, had been observed in QMDH. Notably, the latter *cis*-peptide bond is realised as a structurally equivalent Lys/Trp *cis*-peptide bond in QMDH. This non-Pro *cis*-bond at Tyr289 in QEDH stabilizes a β-turn far away from the active-site. It should be pointed out that non-proline *cis*-peptide bonds are quite rare structural events in enzymes. The two *cis*-Pro peptide bonds at positions 269 and 406 are located in the vicinity of the active-site residues Asn266, Trp270 and Phe408. It may be assumed that these special configurations are necessary for stabilizing the proper conformation of backbone segments around the active-site of the enzymes. A third *cis*-Pro reported for QMDH at position 72 of the enzyme from *M*. W3A1 is not present in QEDH.

Of the 74 water molecules added to subunit A of QEDH, about one-third are at equivalent positions when compared with the QMDH structure of *M*. W3A1. Of these, four are found above the PQQ moiety, not in the active-site cavity but at the opposite site of the disulphide bridge, and two others in the vicinity of Pro267 and Pro311, two residues conserved in QMDH. There is no electron density for any water molecule in the active-site cavity of QEDH.

Additional calcium-binding site

In addition to the metal-binding site present in the active-site cavity of both QEDH and QMDH, where a calcium ion is bound near the prosthetic group PQQ, a second putative metal-binding site was found at the N terminus of QEDH. The ligand sphere is established by Asp11, Thr14 and Asp17, which act as bidentate ligands (Figure 4). Such a 6-fold coordination sphere is often found in proteins for binding calcium ions. Also Ca^{2+} is the only metal ion added to the crystallization setup. The site was tested with water, sodium and calcium ions at the end of the structure refinement and short cycles of further refinement were performed. Of the species tested, only Ca^{2+} had *B*-factor values comparable to those of the ligand atoms. When a water molecule was placed in this site, F_o-F_c electron density was observed.

Previous heat-inactivation experiments with QEDH in the presence and absence of Ca^{2+} revealed a stabilizing effect of this ion [Mutzel and Gorisch 1991]. Apparently, the N-terminal additional Ca^{2+} site identified in QEDH contributes to stabilizing the native conformation of the enzyme.

Subunit interaction

A superposition of both subunits in the final model of QEDH shows an almost identical conformation, with an overall r.m.s. of 0.38 Å. Some minor differences in external loop positions between residues 219-237, 330-334, 392-401, and the N and C terminus may be caused by the scarce information available.

There is an extended interaction area between the two subunits of the stable dimer. The specific contacts are mainly hydrophobic interactions of the residues Pro46/Pro46, Phe523; Ala569/Tyr50; Trp575/Trp575; Trp582/Phe42, Lys43, Pro580, Trp582; and hydrogen bonds between the residues Ser49(CO)/Gly526(NH); Ser49(NH)/Gln524(CO); Ser51(NH)/Gly526(CO); Glu55(OE1)/Tyr77(OH); Gln57(NH); and Gln570(CO)/Ser51(OG). All contacts occur twice due to the symmetry of the interaction. No salt-bridge is involved.

A comparison of the subunit interactions in QMDH and QEDH shows that, despite the identical localization of the interaction surfaces, the residues involved and the types of interactions are not conserved (Scheme 2). Out of nine interactions identified in QEDH, there is only one hydropho-

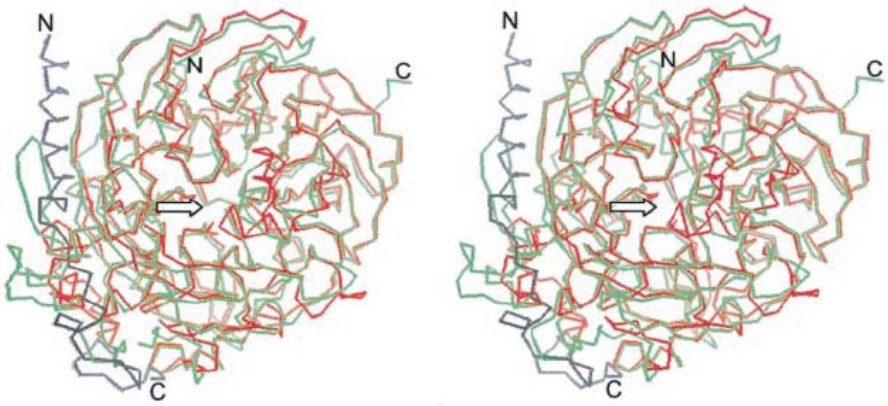

Figure 3. Stereo view of the superposition of QEDH (green) with QMDH of *Methylophilus* W3A1 (large subunit in red, small subunit in grey), only C^{α} atoms are presented. The chain termini are indicated, the active-site region is marked by an arrow.

bic interaction and two hydrogen bridges that are equivalent in QMDH from *M.*W3A1.

Active-site region

In the active-site of QEDH there is clear electron density for the prosthetic group of this enzyme, the tricyclic ring system of PQQ. A metal ion-binding site is comprised by the side-chains of Glu179, Asn266 and Asp316. This site is occupied by a calcium ion, which is also liganded by PQQ *via* O5, N6 and O7A (Figure 5(a). The position of the PQQ group is fixed mainly by a hydrogen bond network including the side-chains of several amino acid residues (Table 2), a hydrophobic interaction with the side-chain of Trp248 beneath in parallel orientation, interaction with the calcium ion, and van der Waals contact with the sulphur atoms of an unusual disulphide bridge between the adjacent Cys105 and Cys106. The residues in contact with the PQQ prosthetic group in QEDH, the ligands of the calcium-binding site, and the unusual disulphide ring are strictly conserved in comparison with QMDH (Scheme 2), the relative positions of these moieties in the corresponding structures being identical within the limit of error in the crystallographic data.

In QMDH, an additional hydrogen bridge established *via* a Thr residue is involved in anchoring PQQ. This Thr of QMDH is exchanged by Ala246 in QEDH. The interaction distances between Ca^{2+} and the ligands of the metal-binding site donated by PQQ are very similar in the QEDH and the QMDH structures; however, they are significantly longer by 0.4 to 0.45 Å than the distances calculated for the Ca^{2+} complex of free PQQ [Zheng and Bruice 1997].

Unlike QMDH, the prosthetic group PQQ of *P. aeruginosa* QEDH dissociates from the enzyme after removal of Ca^{2+} upon treatment with a chelating agent. This process is completely reversible and full activity is restored after reconstitution in the presence of Ca^{2+} and PQQ [Mutzel and Gorisch 1991]. In contrast, PQQ from QMDH can be re-

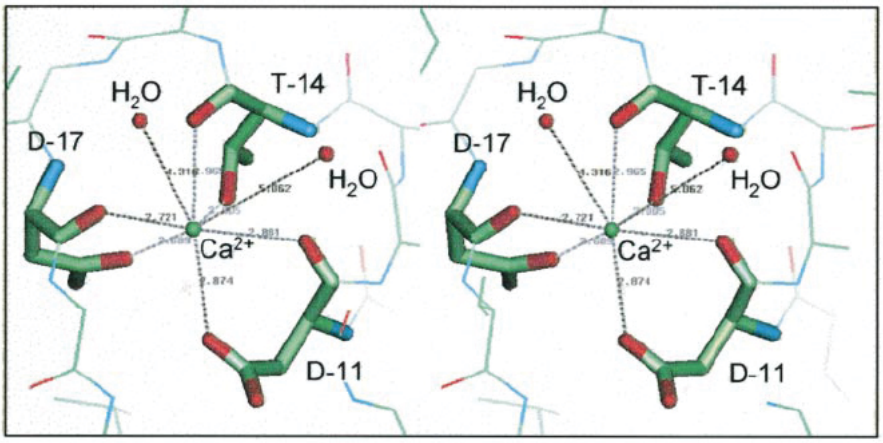

Figure 4. Stereo view of the second calcium-binding site in QEDH from *P. aeruginosa* with the three bidentate ligands Asp11, Thr14 and Asp17, and two neighbouring water molecules; important distances are indicated (in Å).

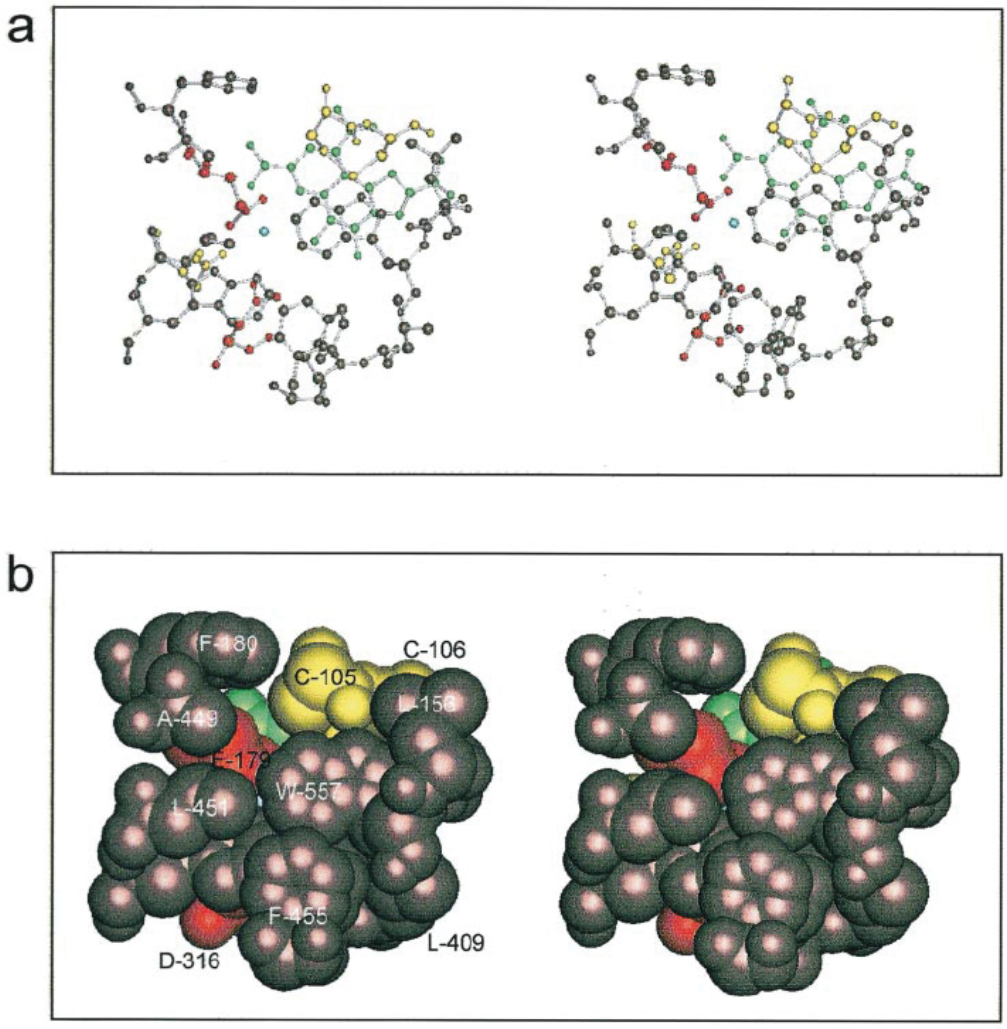

Figure 5. Active-site cavity of QEDH from *P. aeruginosa*, including PQQ and Ca^{2+}, stereo view from the entrance to the active-site. (a) Ball-and-stick representation; (b) space-filling representation. Hydrophobic residues, brown; polar residues, yellow; acidic residues, red; PQQ, green; Ca^{2+}, blue.

moved only by irreversibly denaturing the enzyme [Patel et al 1978 and Davidson et al 1985]. Apparently, the additional disulphide bridge present in the large subunit of QMDH and the complex with the small subunit lead to a strong stabilization of the native conformation of the enzyme.

The tricyclic ring system of PQQ in the active-site of QEDH appears to be almost planar. The quality of the electron density map does not permit us to determine whether the oxygen atoms at C4 or C5 are out of the plane, a situation reported to be the case in both structures of QMDH, where the prosthetic group is in the semiquinone state [Ghosh et al 1995 and Xia et al 1999]. Early electron spin resonance (ESR) studies with QMDH, however, indicated that the spin density is distributed over the tricyclic ring system of PQQ and recent *ab initio* calculations support the view that the free semiquinone radical $PQQH^{\bullet}$ is planar [Zheng and Bruice 1997].

The walls of the active-site cavity in QEDH are formed by several hydrophobic residues, Trp270, Phe408, Leu409 and Ala553. Another tryptophan residue, Trp557 forms a "lid" closing the active-site cavity (Figure 5(a). Trp557 is positioned within a sharp turn including the eight residues from Gly552 to Gly559. The position of the tryptophan lid is stabilized by several hydrophobic contacts with Leu451, Phe455 and Leu556. Access to the substrate cavity is by a funnel-shaped channel formed by the side-chains of Cys105, Glu179, Trp270, Phe408, Ala449, Leu451 and Phe455. The walls of this channel are mainly hydrophobic. Differences in the active-site region between QEDH and QMDH are found with the residues lining the entrance to, and the cavity of, the active-site. One side of the active-site cavity of QMDH is limited by a Trp residue located in a loop connecting β-strands B and C of W_8. In the QEDH amino acid sequence, this Trp is replaced by Ala553. How-

Table 2. List of PQQ interactions within the QEDH structure

Interacting moiety	Nature of contact with PQQ
Ca^{2+}	Coordination (O5, N6, O7A)
Glu61	H bond (O2A)
Cys105	van der Waals
Cys106	van der Waals
Arg111	H bond (O2A, O9B)
Thr155	H bond (O9A)
Ser176	H bond (O9A)
Gly177 (N)	H bond (O7B)
Asp178 (N)	H bond (O7B)
Trp248	Hydrophobic interaction
Arg344	H bond (O4, O5)
Trp489	H bond (O2A)
Ala553 (N)	H bond (O2B)

ever, the structural function of the bulky Trp side-chain in QMDH is supplied in QEDH by Phe408 and Leu409 residing in a loop connecting the β-sheet propellers W_5 and W_6 (Scheme 1 and Scheme 2).

The ceiling of the cavity in QEDH is formed by the lid of the side-chain of Trp557, which covers one half of the active-site. At the Trp557 position there is Leu in QMDH. On the opposite side of the hydrophobic cavity the entrance to the active-site of QEDH is remodelled by Phe180 and Ala449 replacing Leu and Phe in QMDH. Both latter exchanges result in a shift of the aperture of the cavity, thereby causing an increase of the active-site volume in QEDH, but also making the entrance to the active-site cavity considerably narrower.

The surface area around the entrance to the active-site in QEDH shows a slight depression and consists preferentially of the hydrophobic residues Cys105, Phe180, Ala449, Leu451, Phe455, Leu556 and Trp557 (Figure 5(b).

The respective residues in the QMDH sequence, which constitute an equivalent funnel region above the PQQ moiety in QMDH, are also hydrophobic (Scheme 2). Soluble quinoprotein alcohol dehydrogenases transfer their electrons to special *c*-type cytochromes. [Anthony et al 1994] proposed an interaction of QMDH from *M. extorquens* with cytochrome c_L at the hydrophobic funnel region. Cytochrome c_{550}, which accepts electrons from QEDH [Reichmann and Gorisch 1993], however, shares only little sequence homology with cytochrome c_L [Schobert and Gorisch 1999].

Substrate specificity and docking calculations

QEDH and QMDH differ significantly in their substrate specificity, as shown in Table 3 for different alcohols. With respect to secondary alcohols, it has been shown with the enzyme from *M. extorquens (Pseudomonas* M27) that QMDH does not accept secondary alcohols like 2-propanol [Anthony 1986]. The K_m values for ethanol are in the micromolar range for both QEDHs and QMDHs. If methanol is used as a substrate, QMDHs show K_m values in the same concentration range, whereas with QEDHs the K_m values are increased by about three orders of magnitude. The maximum reaction velocities are comparable for both substrates. QEDHs obviously discriminate between methanol and ethanol mainly by affinity, resulting in different catalytic effectivities. With QEDH the affinity for 1-propanol is still comparable to ethanol but for 2-propanol it is remarkably lower, by almost two orders of magnitude. For butanol, the affinity drops by a factor of about 10.

The affinities for different alcohols are expected to correlate with differences in contacts to amino acid residues in the active-site. Docking calculations were performed with methanol, ethanol, 1-propanol, 1-butanol and 2-propanol as substrate of QEDH from *P. aeruginosa*. Since Trp557 forms

Table 3. Kinetic parameters for different QEDHs and QMDHs and various substrates

	QEDH									QMDH					
	Pseudomonas aeruginosa														
	ATCC 17933[a]			BB1[b]			*Rhodopseudomonas acidophila*[c]			*Methylophilus methylotrophus*[d]			*Hyphomicrobium* WC[e]		
Substr.	K_m	V_{max}	K_{eff}	K_m	V_{max}	K_{eff}	K_m	V_{max}	K_{eff}	K_m	V_{max}	K_{eff}	K_m	V_{max}	K_{eff}
M	94	62	0.66	31.7	80	2.5	120	53	0.44	0.02	100	5000	0.014	100	7143
E	0.014	100	7140	0.01	100	10000	0.03	100	3333	0.028	76	2714	0.016	100	6250
1-P	0.021	138	6570	0.008	100	12500	0.04	100	2500	0.28	94	336	0.036	106	2944
2-P	0.68	115	170	2.7	142	52	5.2	96	18.5	n.d.[f]	n.d.		n.d.[f]	n.d.	
1-B	0.37	65	175	n.d.	n.d.		0.4	100	250	0.285	89	312	0.04	100	2500

$K_{eff} = V_{max}/K_m$; K_m (mM); relative V_{max} with V_{max} for methanol or ethanol set to 100%.
Substr., Substrate; M, methanol; E, ethanol; 1-P, 1-propanol; 2-P, 2-propanol; 1-B, 1-butanol.
[a] Görisch & Rupp (1989); sequence known: Diehl *et al.* (1998); structure: this work.
[b] Dijkstra *et al.* (1985).
[c] Sahm *et al.* (1976).
[d] Ghosh & Quayle (1981); sequence and structure of *Methylophilus* W3A1 known: Xia *et al.* (1996).
[e] Sperl *et al.* (1974).
[f] In other studies with QMDH it was shown that 2-propanol is not accepted as substrate (Anthony, 1986).

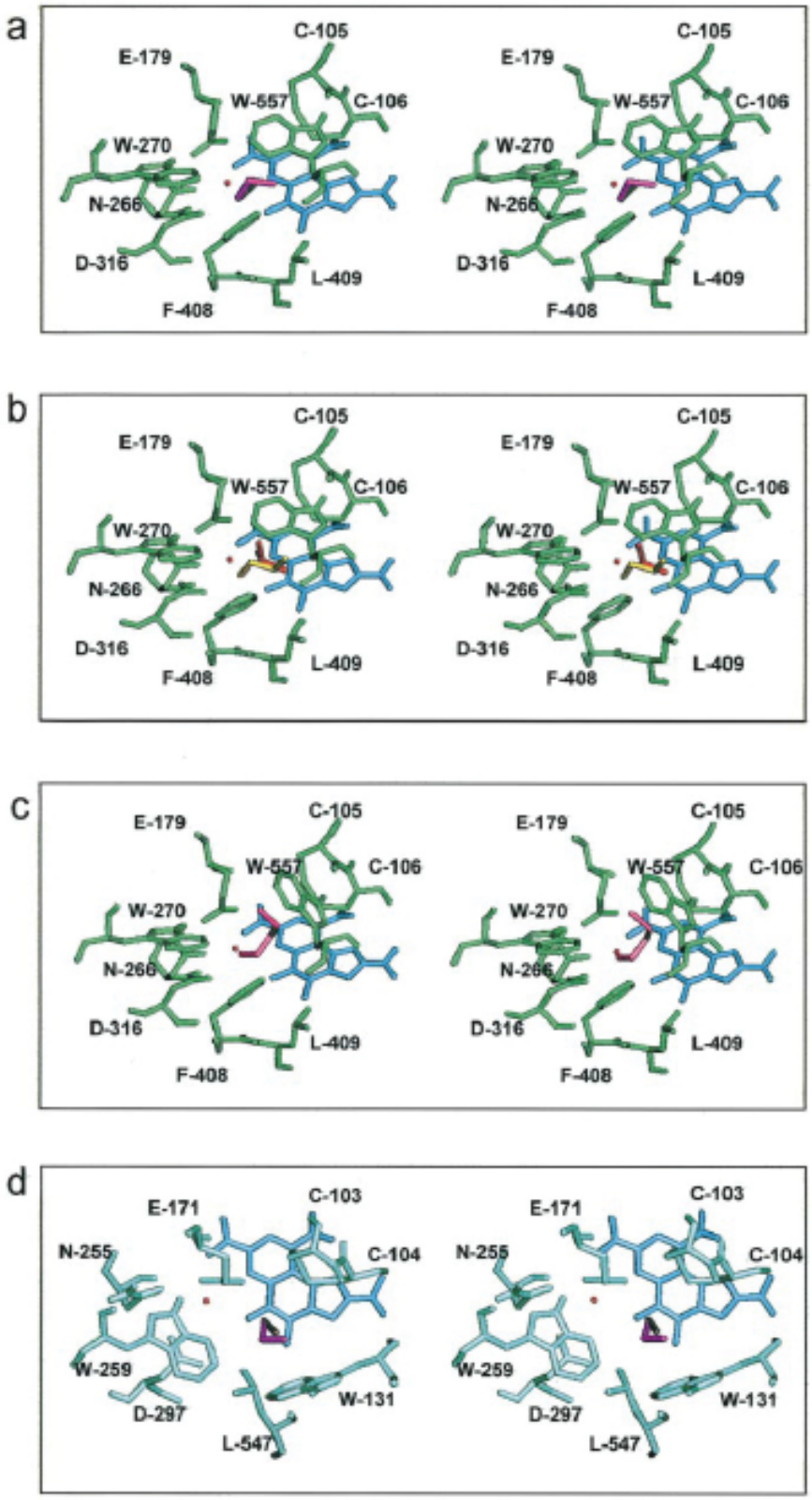

Figure 6. Stereo view of docking different alcohol substrates to the active-site of QEDH from *P. aeruginosa* or QMDH from *M*. W3A1. The OH groups of the substrates point away from the viewer towards the Ca^{2+} underneath. Polar hydrogen atoms like the indole NH are included in docking calculations and are shown (a) QEDH with methanol (grey) and ethanol (purple). (b) QEDH with 1-propanol (yellow) and 2-propanol (orange). (c) QEDH with 1-butanol (pink). (d) QMDH with methanol (grey) and ethanol (purple). QEDH residues, green; QMDH residues, light blue; PQQ, blue; Ca^{2+}, red.

a lid-like cover in the native structure of QEDH, prohibiting immediate access to the proposed reaction site, the Trp side-chain was tilted out of its given position by means of changing the χ_2 angle by about 70 °. In the resulting funnel, the respective alcohol molecules were placed with the hydroxyl group pointing into the interior of the enzyme but at a distance from the putative reaction center (O_{alc}–$O4_{PQQ}$~7 Å, O_{alc}–Ca^{2+}~6 Å). In these docking calculations, the oxidized form of PQQ was used. For comparison, similar calculations were done for QMDH from *M*. W3A1 with methanol and ethanol. The resulting structures of the complexes with lowest energy are shown in Figure 6(a)–(d).

In the case of QEDH, the docking calculations for methanol, ethanol and 1-propanol result in quite similar orientations of the alcoholic OH group pointing towards the Asp316 carboxyl group *via* a hydrogen bridge (Figure 6(a). This residue is present in QMDH and, interestingly, it was suggested to be involved in proton abstraction from the alcohol *via* an initial hydrogen bridge [Anthony 1996], a mechanistic aspect that is supported by our docking calculations. The clearly unfavourable orientation of 2-propanol, with its OH group pointing towards the O5 atom of PQQ (Figure 6(b), is in agreement with the observed lower affinity compared to 1-propanol (Table 3). In order to fit 1-butanol or higher alcohols with more than four carbon atoms into the active-site of QEDH, a flip of the Trp557 side-chain orientation is necessary, otherwise the active-site cavity is not large enough (Figure 6(c). This flip of Trp557 might be the cause for the less favourable K_m values found with higher primary alcohols.

The docking calculations provide evidence for a less favourable binding of methanol compared to ethanol in the active-site of QEDH. While ethanol is encased by residues Cys105, Cys106, Glu179, Trp270, Asp316, Arg344, Phe408 and Trp557 with close van der Waals contacts to Cys106, Asp316, Phe408 and the prosthetic group PQQ, methanol is bound rather loosely by direct van der Waals contact only to Asp316 and PQQ (Figure 6(a). The lesser number of contacts involved in binding methanol in contrast to ethanol might explain the difference in K_m values for these substrates found with QEDH.

In the active-site of QMDH, both methanol and ethanol are embedded by close van der Waals contacts with the surrounding amino acid residues. In the *M*. W3A1 sequence, these are residues Cys104, Cys105, Glu171, Trp531, Leu547 and the PQQ molecule (Figure 6(d), where among the methanol contacts Trp531 may play an essential role. The same number of contacts in QMDH involved in binding methanol and ethanol explains why this enzyme shows similar K_m values for both substrates.

Recently, the structure analysis of another crystal form of QMDH from *M*. W3A1 revealed a difference electron density in the active-site compatible with methanol [Xia et al 1999]. The position and orientation of the substrate in this structure is very close to that found for QMDH in our docking calculations, thus supporting the results obtained by the docking procedure applied.

Conclusion

The QEDH structure described here, despite being very similar to the reported QMDH structures, shows some remarkable differences, like a set of larger external loops instead of the presence of a small subunit, and an additional calcium-binding site at the N terminus, which increases the stability of the enzyme. The differences in substrate specificity of QEDH and QMDH may be attributed to differences in amino acid side-chains lining the active-site cavity and the entrance to the active-site.

The question of how electron transfer from the reduced PQQ to the respective cytochromes is accomplished, as well as elucidation of the full reaction cycle of PQQ-dependent alcohol dehydrogenases can be solved only by structural analyses of a complex between these proteins, work that is now in progress in our laboratories with QEDH and cytochrome c_{550}.

Materials and methods

QEDH from *P. aeruginosa* ATCC 17933 was purified as described [Rupp and Gorisch 1988].

Crystallization and data collection

Crystals were obtained from hanging drop crystallization setups with 10 % (w/v) PEG 1500, 4.5 mM glycine/NaOH (pH 8.0), 50 mM $CaCl_2$ at room temperature [Rupp and Gorisch 1988 and Stezowski et al 1989].

X-ray diffraction data were collected at the X31 synchroton radiation beamline of the EMBL outstation (DESY, Hamburg, Germany) from a single crystal at room temperature on a MarResearch area detector (Hamburg, Germany). Reflections were integrated, scaled and reduced by using MOSFLM [Leslie 1990] and programs from the CCP4 suite [Collaborative Computational Project 1994].

Structure determination

The method of molecular replacement was applied and the model chosen for solving the rotation and translation in AMoRe [Navaza et al 1998] was a large subunit of the heterotetrameric QMDH from *Methylophilus*W3A1 [Xia et al 1992] with the RCSB protein data bank identity code 4aah.

At early stages, the QEDH dimer model was refined with X-PLOR [Brunger 1992] with strict NCS applied and coordinates being inspected and manually rebuilt by using

O [Jones et al 1991]. The electron densities were subjected to density modification (solvent flattening, histogram matching) performed by DM [Cowtan and Main 1993].

At later stages, only REFMAC (CCP4, 1994) was used for refinement with and without non-crystallographic symmetry (NCS). Areas important for structure model interpretation or loop areas that tend to have different conformations in both monomer molecules were checked with omit electron density maps.

The stereochemistry of the model was monitored by PROCHECK [Laskowski et al 1996].

Docking calculations

The software package ICM (Internal Coordinate Mechanics, [Abagyan et al 1994]) was used for docking experiments with different alcohols. First, the crystal structures of QEDH and QMDH from *M.* W3A1 (identification code 4aah) were regularized to produce a full-atom model with idealized covalent geometry as close as possible to the given Cartesian coordinates. Monte-Carlo simulations were performed to obtain the optimal alcohol positions. The enzyme amino acid side-chains in a 6 Å environment of the alcohols were considered flexible and sampled together with the translational/rotational and internal degrees of freedom of the respective alcohol. The temperature used in the Metropolis criterion [Metropolis et al 1953] was set to 700 K but allowed to increase in the case of a conformation becoming overvisited; dislocation of the centre of mass of the alcohols of up to 10 Å was not penalized. A total of 10^5 function calls were invoked for each simulation that included up to 100 minimization steps after each random move. The calculations were monitored by recording a stack of 50 low-energy conformations [Abagyan and Argos 1992].

Protein data bank accession number

Atom coordinates for the protein structure reported here are deposited in the RCSB Protein Data Bank under accession number 1EEE.

Acknowledgements

The authors thank G. Zahn and Dr B. Kallies for their help in the docking calculations, and Dr M. Hahn for critical reading of the manuscript, Dr J. Ay supported the secondary structure assignment. We thank C. Anthony, University of Southampton, for making available to us the atomic coordinates of QMDH from *M. extorquens,* and Dr Z. Dauter, EMBL Hamburg, for help in data collection and processing.

References

Abagyan, R. A., and P. Argos (1992). Optimal protocol and trajectory visualization for conformational searches of peptides and proteins. *J. Mol. Biol.* **225**, pp. 519–532.

Abagyan, R. A., M. M. Totrov, and D. N. Kuznetsov (1994). ICM—a new method for protein modeling and design. Applications to docking and structure prediction from the distorted native conformation. *J. Comput. Chem.* **15**, pp. 488–506.

Anthony, C. (1986). Bacterial oxidation of methane and methanol. *Advan. Microbial. Physiol.* **27**, pp. 113–210.

Anthony, C. (1993). Methanol dehydrogenase in gram-negative bacteria. In: V.L. Davidson, Editor, *Principles and Application of Quinoproteins*, Marcel Dekker, New York, pp. 17–45.

Anthony, C. (1996). Quinoprotein-catalysed reactions. *Biochem. J.* **320**, pp. 697–711.

Anthony, C., and M. Ghosh (1998). The structure and function of the PQQ-containing quinoprotein dehydrogenases. *Prog. Biophys. Mol. Biol.* **69**, pp. 1–21.

Anthony, C., M. Ghosh, and C. C. Blake (1994). The structure and function of methanol dehydrogenase and related quinoproteins containing pyrrolo-quinoline quinone. *Biochem. J.* **304**, pp. 665–674.

Baker, S. C., N. F. Saunders, A. C. Willis, S. J. Ferguson, J. Hajdu, and V. Fulop (1997). Cytochrome cd_1 structure: unusual haem environments in a nitrite reductase and analysis of factors contributing to β-propeller folds. *J. Mol. Biol.* **269**, pp. 440–455.

Bamforth, C. W., and J. R. Quayle (1979). Structural aspects of the dye-linked alcohol dehydrogenase of *Rhodopseudomonas acidophila*. *Biochem. J.* **181**, pp. 517–524.

Branden, C., and J. Tooze (1991). *Introduction to Protein Structure*, Garland Publishing Co., New York.

Brünger, A. T. (1992). *X-PLOR, Version 3.0: A System for X-ray and NMR*, Yale University Press, New Haven, CT.

Collaborative Computational Project (1994). *The CCP4 Suite: Programs for Protein Crystallography*, SERC Daresbury Laboratory, Warrington WA4 4AD England.

Cowtan, K. D., and P. Main (1993). Improvement of macromolecular density maps by the simultaneous application of real and reciprocal space constraints. *Acta Crystallog. sect. D* **49**, pp. 148–157.

Cozier, G. E., I. G. Giles, and C. Anthony (1995). The structure of the quinoprotein alcohol dehydrogenase of *Acetobacter aceti* modelled on that of methanol dehydrogenase from *Methylobacterium extorquens*. *Biochem. J.* **308**, pp. 375-279 .

Davidson, V. L., J. W. Neher, and G. Cecchini (1985). The biosynthesis and assembly of methanol dehydrogenase in bacterium W3A1. *J. Biol. Chem.* **260**, pp. 9642–9647.

de Jong, G. A., A. Geerlof, J. Stoorvogel, J.A. Jongejan, S. de Vries, and J.A. Duine (1995). Quinoheamoprotein ethanol dehydrogenase from *Comamonas testosteroni*. Purification, characterization, and reconstitution of the apoenzyme with pyrroloquinoline quinone analogues. *Eur. J. Biochem.* **230**, pp. 899–905.

Diehl, A.V., F. Wintzingerode, and H. Görisch (1998). Quinoprotein ethanol dehydrogenase of *Pseudomonas aeruginosa* is a homodimer. Sequence of the gene and deduced structural properties of the enzyme. *Eur. J. Biochem.* **257**, pp. 409–419.

Dijkstra, M., W. J. J. van den Tweel, J. A. M. de Bont, J. Frank, and J.A. Duine (1985). Monomeric and dimeric quinoprotein alcohol dehydrogenase from alcohol-grown *Pseudomonas*-BB1. *J. Gen. Microbiol.* **131**, pp. 3163–3169.

Geiger, O., and H. Görisch (1989). Reversible thermal inactivation of the quinoprotein glucose dehydrogenase from *Acinetobacter calcoaceticus*. *Biochem. J.* **261**, pp. 415–421.

Ghosh, R., and J.R. Quayle (1981). Purification and properties of the methanol dehydrogenase from *Methylophilus methylotrophus*. *Biochem. J.* **199**, pp. 245–250.

Ghosh, M., A. Avezoux, C. Anthony, K. Harlos, and C.C. Blake (1994). X-ray structure of PQQ-dependent methanol dehydrogenase. *EXS* **71**, pp. 251–260.

Ghosh, M., C. Anthony, K. Harlos, M.G. Goodwin, and C. Blake (1995). The refined structure of the quinoprotein methanol dehydrogenase from *Methylobacterium extorquens*. *Structure* **3**, pp. 177–187.

Gomis, R. F., U. Gohlke, M. Betz, V. Knauper, G. Murphy, O.C. Lopez, and W. Bode (1996). The helping hand of collagenase-3 (MMP-13): 2.7 A crystal structure of its C-terminal haemopexin-like domain. *J. Mol. Biol.* **264**, pp. 556–566.

Goodwin, P. M., and C. Anthony (1998). The biochemistry, physiology and genetics of PQQ and PQQ containing enzymes. *Advan. Microb. Physiol.* **40**, pp. 1–80.

Görisch, H., and M. Rupp (1989). Quinoprotein ethanol dehydrogenase from *Pseudomonas*. *Antonie van Leeuwenhoek* **56**, pp. 35–45.

Janakiraman, M. N., C. L. White, W. G. Laver, G. M. Air, and M. Luo (1994). Structure of influenza virus neuraminidase B/Lee/40 complexed with sialic acid and a dehydro analog at 1.8-Å resolution: implications for the catalytic mechanism. *Biochemistry* **33**, pp. 8172–8179.

Jones, T. A., J. Y. Zou, S. W. Cowan, and Kjeldgaard (1991). Improved methods for binding protein models in electron density maps and the location of errors in these models. *Acta Crystallog. sect. A* **47**, pp. 110–119.

Jongejan, A., J. A. Jongejan, and J. A. Duine (1998). Homology model of the quinohaemoprotein alcohol dehydrogenase from *Comamonas testosteroni*. *Protein Eng.* **11**, pp. 185–198.

Laskowski, R. A., J. M. Thornton, C. Humblet, and J. Singh (1996). X-SITE: use of empirically derived atomic packing preferences to identify favourable interaction regions in the binding sites of proteins. *J. Mol. Biol.* **259**, pp. 175–201.

Leslie, R. (1990). *Crystallographic Computing*, Oxford University Press, Oxford.

Matsushita, K., and O. Adachi (1993). Bacterial quinoproteins glucose dehydrogenase and alcohol dehydrogenase. In: V. L. Davidson, Editor, *Principles and Application of Quinoproteins*, Marcel Dekker, New York, pp. 47–63.

Metropolis, N., A. W. Rosenbluth, M. N. Rosenbluth, A. H. Teller, and E. Teller (1953). Equation of state calculations by fast computing machines. *J. Chem. Phys.* **21**, pp. 1087–1092.

Murzin, A. G. (1992). Structural principles for the propeller assembly of beta-sheets: the preference for seven-fold symmetry. *Proteins: Struct. Funct. Genet.* **14**, pp. 191–201.

Mutzel, A., and H. Görisch (1991). Quinoprotein ethanol dehydrogenase: preparation of the apo-form and reconstitution with pyrroloquinoline quinone and Ca^{2+} or Sr^{2+} ions. *Agric. Biol. Chem.* **55**, pp. 1721–1726.

Navaza, J., E. H. Panepucci, and C. Martin (1998). On the use of strong Patterson function signals in many-body molecular replacement. *Acta Crystallog. sect. D* **54**, pp. 817–821.

Nunn, D. N., D. Day, and C. Anthony (1989). The second subunit of methanol dehydrogenase of *Methylobacterium extorquens* AM1. *Biochem. J.* **260**, pp. 857–862.

Patel, R. N., C. T. Hou, and A. Felix (1978). Microbial oxidation of methane and methanol: crystallization of methanol dehydrogenase and properties of holo- and apo-methanol dehydrogenase from *Methylomonas methanica*. *J. Bacteriol.* **133**, pp. 641–649.

Ramachandran, G. N., and V. Sasisekharan (1968). Conformation of polypeptides and proteins. *Advan. Protein. Chem.* **23**, pp. 283–438.

Reichmann, P., and H. Görisch (1993). Cytochrome c_{550} from *Pseudomonas aeruginosa*. *Biochem. J.* **289**, pp. 173–198.

Renault, L., N. Nassar, I. Vetter, J. Becker, C. Klebe, M. Roth and A. Wittinghofer (1998). The 1.7 Å crystal structure of the regulator of chromosome condensation (RCC1) reveals a seven-bladed propeller. *Nature* **392**, pp. 97–101.

Rupp, M., and H. Görisch (1988). Purification, crystallization and characterization of quinoprotein ethanol dehydrogenase from *Pseudomonas aeruginosa*. *Biol. Chem. Hoppe Seyler* **369**, pp. 431–439.

Sahm, H., R. B. Cox, and J. R. Quayle (1976). Metabolism of methanol by *Rhodopseudomonas acidophila*. *J. Gen. Microbiol.* **94**, pp. 313–322.

Schobert, M., and H. Görisch (1999). Cytochrome c_{550} is an essential component of the quinoprotein ethanol oxidation system in *Pseudomonas aeruginosa*: cloning and sequencing of the genes encoding cytochrome c_{550} and an adjacent acetaldehyde dehydrogenase. *Microbiology* **145**, pp. 471–481.

Schrover, J. M., J. Frank, J. E. van Wielink, and J.A. Duine (1993). Quaternary structure of quinoprotein ethanol dehydrogenase from *Pseudomonas aeruginosa* and its reoxidation with a novel cytochrome *c* from this organism. *Biochem. J.* **290**, pp. 123–127.

Shimao, M., K. Ninomiya, O. Kuno, N. Kato and C. Sakazawa (1986). Existence of a novel enzyme, pyrroloquinoline quinone-dependent polyvinyl alcohol dehydrogenase, in a bacterial symbiont, *Pseudomonas* sp. strain VM15C. *Appl. Environ. Microbiol.* **51**, pp. 268–275.

Sperl, G. T., H. S. Forrest, and D. T. Gibson (1974). Substrate specificity of the purified primary alcohol dehydrogenases from methanol-oxidizing bacteria. *J. Bacteriol.* **118**, pp. 541–550.

Stezowski, J. J., H. Görisch, Z. Dauter, M. Rupp, A. Hoh, R.

Englmaier, and K. Wilson (1989). Preliminary X-ray crystallographic study of quinoprotein ethanol dehydrogenase from *Pseudomonas aeruginosa*. *J. Mol. Biol.* **205**, pp. 617–618.

Toyama, H., A. Fujii, K. Matsushita, E. Shinagawa, M. Ameyama, and O. Adachi (1995). Three distinct quinoprotein alcohol dehydrogenases are expressed when *Pseudomonas putida* is grown on different alcohols. *J. Bacteriol.* **177**, pp. 2442–2450.

van Kleef, M. A., and J.A. Duine (1988). Bacterial NAD(P)-independent quinate dehydrogenase is a quinoprotein. *Arch. Microbiol.* **150**, pp. 32–36.

White, S., G. Boyd, F.S. Mathews, Z. X. Xia, W.W. Dai, Y. F. Zhang, and V. L. Davidson (1993). The active-site structure of the Ca-containing quinoprotein methanol dehydrogenase. *Biochemistry* **32**, pp. 12955–12958.

Xia, Z. X., W. W. Dai, J. P. Xiong, Z. P. Hao, V. L. Davidson, S. White, and F. S. Mathews (1992). The three-dimensional structures of methanol dehydrogenase from two methylotrophic bacteria at 2.6-Å resolution. *J. Biol. Chem.* **267**, pp. 22289–22297.

Xia, Z., W. Dai, Y. Zhang, S. A. White, G. D. Boyd, and F. S. Mathews (1996). Determination of the gene sequence and the three-dimensional structure at 2.4 Å resolution of methanol dehydrogenase from *Methylophilus* W3A1. *J. Mol. Biol.* **259**, pp. 480–501.

Xia, Z. X., Y. N. He, W. W. Dai, S. A. White, G. D. Boyd, and F. S. Mathews (1999). Detailed active-site configuration of a new crystal form of methanol dehydrogenase from *Methylophilus* W3A1 at 1.9 Å resolution. *Biochemistry* **38**, pp. 1214–1220.

Zheng, Y. J., and T.C. Bruice (1997). Conformation of coenzyme pyrroloquinoline quinone and role of Ca^{2+} in the catalytic mechanism of quinoprotein methanol dehydrogenase. *Proc. Natl Acad. Sci. USA* **94**, pp. 11881–11886.